Modulation of Human Nucleotide Excision Repair by 5-Methylcytosines†

Regula Muheim,‡ Tonko Buterin,‡ Katharine C. Colgate,§ Alexander Kolbanovsij,§ Nicholas E. Geacintov,§ and Hanspeter Naegeli*,‡

Institute of Pharmacology and Toxicology, University of Zürich-Tierspital, 8057 Zürich, Switzerland, and Chemistry Department, New York University, New York, New York 10003

Received September 13, 2002; Revised Manuscript Received December 23, 2002

ABSTRACT: Previous reports showed that methylated CpG sites are primary targets of bulky lesions induced by UV radiation, benzo[*a*]pyrene (B[*a*]P), or other environmental genotoxic agents. This study was performed to determine whether the repair of DNA damage formed preferentially at CpG dinucleotides is sensitive to 5-methylcytosine substitutions. Reactivation assays using UV- or B[*a*]P diol epoxide-damaged shuttle vectors established that human nucleotide excision repair enzymes are able to process fully methylated target DNA molecules. Repair reactions in human cell extracts suggested that 5-methylcytosines modulate local repair efficiency in a seemingly unpredictable manner. In fact, excision of the predominant (+)-*trans*-*anti*-B[*a*]P−dG adduct situated in a mutational hot spot sequence (codon 273 of the *p53* gene) was stimulated by CpG methylation. Interestingly, excision activity was increased by a single 5-methylcytosine residue flanking the adduct in the damaged strand, but the same stimulatory effect was also induced by a single 5-methylcytosine residue located opposite the adduct in the undamaged strand. No such stimulation was observed when the (+)-*trans*-*anti*-B[*a*]P−dG lesion was placed in a different site containing a sequence of contiguous guanines, and strong inhibition was detected when a representative of the rare (+)-*cis*-*anti*-B[*a*]P−dG isomer was tested in the same assay. These results raise the possibility that 5-methylcytosines in CpG dinucleotides modulate not only the distribution of bulky DNA lesions but, at least in some cases, also the kinetics of subsequent excision repair reactions. This study confirms that the efficiency of bulky lesion repair is determined by the configuration of base pairs at damaged sites.

Mammalian DNA methylation patterns are generated by 5-methylcytosine modifications in approximately 70−80% of CpG dinucleotides (*1*−*3*). Previous reports showed that certain bulky base adducts are preferentially induced at CpG sequences and that such a predisposition for damage formation is partly attributable to the presence of 5-methylcytosines instead of cytosines in these critical target sites. An example is provided by the tobacco smoke contaminant benzo[*a*]pyrene (B[*a*]P),[1] which is activated to the ultimate carcinogenic metabolite B[*a*]P diol epoxide leading mainly to (+)-*trans*-*anti*-B[*a*]P adducts at the N^2 position of guanines (*4*, *5*). The distribution of B[*a*]P lesions in human genes is influenced by DNA methylation because the presence of 5-methylcytosine in CpG dinucleotides increases the reactivity of B[*a*]P diol epoxides with the neighboring guanine, thus inducing hot spots for B[*a*]P binding (*6*, *7*). Similarly, the model carcinogen acetylaminofluorene (AAF) is activated to form sulfate or acetate derivatives that react with DNA mainly at the C^8 position of guanine (*8*, *9*). Because the ultimate metabolite *N*-acetoxy-2-AAF binds more efficiently to methylated than to unmethylated CpG dinucleotides, the distribution of AAF−C^8-dG lesions in human DNA sequences is again altered by cytosine methylation (*10*). Another study showed that 5-methylcytosines located in CpG dinucleotides generate preferred target sites for the induction of cyclobutane pyrimidine dimers (CPDs) when DNA is irradiated with natural sunlight (*11*).

To cope with DNA damage arising from chemical carcinogens or UV radiation, mammalian cells are equipped with a versatile DNA repair system that is specialized for the removal of bulky base lesions (*12*−*15*). This DNA damage processing pathway has been termed nucleotide excision repair (NER) because it operates through direct removal of damaged nucleotides by double endonucleolytic cleavage of phosphodiester bonds. One DNA incision occurs on the side 3′ to the lesion and the other on the 5′ side, thus releasing DNA damage as the component of single-stranded oligonucleotide segments (*16*−*18*). The excised DNA oligomers, extending over a length of 24−32 nucleotides in human cells, are replaced by repair patches that are eventually ligated to the preexisting strands (*19*, *20*). Previous findings showing that many NER substrates are preferentially formed at methylated CpG dinucleotides prompted us to test whether NER activity is regulated by 5-methylcytosine substitutions. Thus, we made use of two different assays to determine human NER efficiency in methylated CpG sequences.

† Supported by Swiss National Science Foundation Grant 31-61494.00, by the Krebsliga of the Kanton Zürich (to H.N.), and by NIH/NCI Grant CA 76660 (N.E.G.).

* To whom correspondence should be addressed. Telephone: +41-1-635 87 63. Fax: +41-1-635 89 10. E-mail: naegelih@vetpharm.unizh.ch.

‡ University of Zürich-Tierspital.

§ New York University.

[1] Abbreviations: B[*a*]P, benzo[*a*]pyrene; HPLC, high-performance liquid chromatography; NER, nucleotide excision repair; SAM, *S*-adenosylmethionine; SV40, simian virus 40.

10.1021/bi0268504 CCC: $25.00
Published on Web 02/27/2003

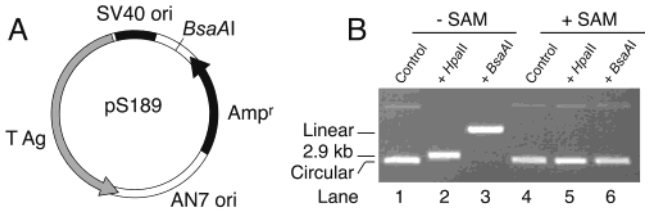

FIGURE 1: Methylation of pS189 plasmid DNA. (A) Schematic representation of the SV40-based construct used for NER-dependent reactivation assays. (B) Restriction analysis demonstrating complete methylation of pS189 DNA after incubation with *Sss*I methylase and *S*-adenosylmethionine (SAM). Lanes 1 and 4 show control samples that were not treated with restriction enzymes.

MATERIALS AND METHODS

Methylation of Shuttle Vectors. Plasmid pS189 (*21*) contains the complete simian virus 40 (SV40) early region, a bacterial origin of replication, and the β-lactamase (Amp^r) gene for selection in bacteria (Figure 1A). This shuttle vector was methylated *in vitro* using the CpG-specific *Sss*I methylase (New England Biolabs) according to the manufacturer's instructions. Control DNA was mock methylated in the absence of *S*-adenosylmethionine (SAM). Complete methylation was confirmed by the resistance of reaction products to digestion by *Bsa*AI and *Hpa*II. Alternatively, effective methylation was demonstrated by the poor yield of colonies observed when methylated plasmids were used to transform Mcr$^+$ Mrr$^+$ *Escherichia coli* strain DH5α (Gibco).

Genotoxic Reactions. UV irradiation of unmethylated or methylated shuttle vector pS189 was performed in 20 μL aliquots containing 2 μg of DNA, 10 mM Tris-HCl (pH 8.0), and 1 mM EDTA, under a germicidal lamp with peak output at 254 nm. Unmethylated or methylated pS189 DNA (333 μg/mL) was modified with racemic 7(*R*),8(*S*)-dihydroxy-9(*S*),10(*R*)-epoxy-7,8,9,10-tetrahydro-B[*a*]P (NCI chemical carcinogen repository; between 20 and 80 μM) in 10 mM Tris-HCl (pH 8.0) and 1 mM EDTA. After incubation for 90 min at 37 °C, the plasmids were precipitated with ethanol and purified by CsCl gradient centrifugation.

Cell Culture and Reactivation Assay. SV40-transformed human fibroblasts (GM00637 and GM04312C) were purchased from the Coriell Institute for Medical Research (Camden, NJ) and grown in Dulbecco's modified Eagle's medium supplemented with 10% fetal calf serum. Prior to each experiment, cells were seeded into 35 mm wells until the cultures reached 50% confluence. The pS189 vector (0.25 μg of DNA per well) was transfected using the Lipofectamine Plus reagent from Invitrogen. Cells were harvested 72 h later and subjected to alkaline lysis, and progeny plasmids were isolated using QIAprep spin columns (Qiagen). The DNA was treated with *Dpn*I (New England Biolabs) to digest any plasmids that still had the bacterial methylation pattern and ensure that all the DNA isolate resulted from replication in human cells. An aliquot of the *Dpn*I digest was directly transformed into competent *E. coli* DH10B or DH5α cells. Transformants were plated onto LB agar plates containing ampicillin (100 μg/mL), and replication efficiency was determined by counting the number of antibiotic-resistant colonies obtained from each 35 mm well.

Internally Labeled Substrates. B[*a*]P−dG adducts were generated by reacting oligonucleotide 5′-GTGCGTGTTTCC-3′, 5′-GTG[^{m}C]GTGTTTCC-3′ (containing a 5-methylcytosine residue in the CpG site), 5′-ATACCCGGGACATC-3′, or 5′-CCATCGCTACC-3′ with racemic 7(*R*),8(*S*)-dihydroxy-9(*S*),10(*R*)-epoxy-7,8,9,10-tetrahydro-B[*a*]P, followed by the purification of singly modified products using reverse-phase high-performance liquid chromatography (HPLC) as described in detail elsewhere (*22*, *23*). Briefly, the initial separation was performed using a Hypersil (Phenomenex, 250 mm × 10 mm) column with an elution profile of 18 to 30% (v/v) methanol in 25 mM phosphate buffer (at 2 mL/min for 90 min). Individual adducted products were purified using a Microsorb C18 (Varian, 250 mm × 4.6 mm) column with an elution profile of 11 to 15% (v/v) acetonitrile in 20 mM triethylamine ethyl acetate buffer (at 1 mL/min for 60 min). Site-specific modifications were confirmed by sequencing the oligonucleotides according to the method of Maxam and Gilbert (*24*). To establish the stereochemical identity of the chromatographic fractions, the samples were enzymatically digested to the nucleoside level with snake venom phosphodiesterase and bacterial alkaline phosphatase. The stereochemistry of each modified 2′-deoxyguanosine was established by HPLC and circular dichroism using appropriate standards (*23*). The purified oligonucleotides were 5′ end-labeled using [γ-^{32}P]ATP (7000 Ci/mmol; ICN Pharmaceuticals) and mixed with five other partially overlapping oligonucleotides that were phosphorylated with cold ATP. The oligonucleotides were annealed and ligated in the presence of T4 DNA ligase, followed by electrophoretic purification of the full-length fragments of 139−142 base pairs as described previously (*25*, *26*).

Excision Assay. Extracts were prepared from HeLa cells as described previously (*27*). Repair reactions (25 μL) were performed with 80 μg of cell extract proteins, internally labeled DNA substrate (0.2 nM, 75 000 dpm), 35 mM HEPES (pH 7.9), 60 mM KCl, 40 mM NaCl, 5.6 mM $MgCl_2$, 0.8 mM dithiothreitol, 0.4 mM EDTA, 3.4% (v/v) glycerol, 2 mM ATP, dATP, dCTP, dGTP, and TTP (80 μM each), and 5 μg of bovine serum albumin. After incubation at 30 °C for 40 min, reactions were stopped by the addition of sodium dodecyl sulfate to 0.3% (w/v) and proteinase K to 200 μg/mL, followed by digestion with proteinase K for 15 min at 37 °C (*24*). DNA was extracted and resolved under denaturing conditions on 10% polyacrylamide gels. After electrophoresis, the dried gels were exposed to X-ray films, and oligonucleotide excision was quantified by scanning the autoradiogram using a Molecular Dynamics computing densitometer equipped with ImageQuant software.

RESULTS

Reactivation of Damaged Viral Vectors in Human Fibroblasts. The shuttle vector pS189 contains both the simian virus 40 (SV40) origin for replication in human cells and the prokaryotic AN7 origin for propagation in bacteria (Figure 1A). An aliquot of the vector was subjected to methylation of CpG dinucleotides using recombinant *Sss*I methylase. To monitor the degree of DNA methylation, we exploited the methylation-sensitive restriction enzymes *Hpa*II and *Bsa*AI, whose recognition sequences contain a CpG site. *Hpa*II cleaves pS189 DNA 13 times at the sequence 5′-CCGG-3′, while *Bsa*AI cleaves pS189 only once in the sequence 5′-PyACGTPu-3′ (where Py and Pu indicate a pyrimidine and a purine base, respectively). When *S*-adenosylmethionine (SAM) was omitted from the incubation

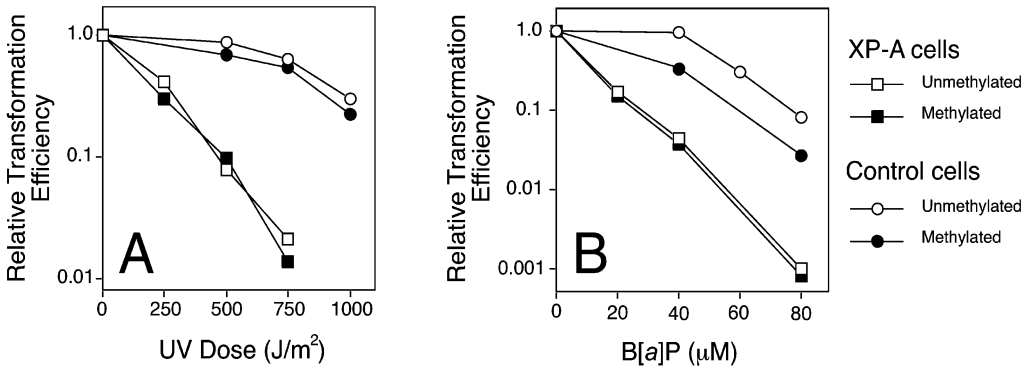

FIGURE 2: Yield of plasmids after replication in human fibroblasts, as estimated from the relative frequency of transformation of bacteria to ampicillin resistance. The plasmid DNA was methylated before exposure to DNA damaging agents. (A) Recovery of transforming DNA as a function of UV dose to the plasmid. For XP-A cells, reactivation was tested in NER-deficient fibroblasts; for control cells, reactivation was tested in NER-proficient fibroblasts. (B) Yield of transforming DNA as a function of B[*a*]P diol epoxide concentration during pretreatment of the plasmids. The reactivation assay was performed in XP-A and control fibroblasts.

with *Sss*I methylase, the pS189 DNA remained unmethylated and, as a consequence, was digested by *Hpa*II, yielding one large DNA fragment of 2883 base pairs (Figure 1B, lane 2). Similarly, *Bsa*AI was able to cleave unmethylated pS189 DNA, generating linearized plasmids (lane 3). When the reaction with *Sss*I methylase was performed in the presence of SAM, both restrictions were completely inhibited (Figure 1B, lanes 5 and 6), indicating that the shuttle vector was methylated at all CpG sites.

Unmethylated and methylated pS189 vectors were exposed to UV-C radiation and subsequently transfected into SV40-transformed human fibroblasts that display different NER capabilities. These human cell lines were derived from healthy individuals (GM00637) or from xeroderma pigmentosum complementation group A (XP-A) patients deficient in NER activity (GM04312C). After transfection with viral vectors, the cells were maintained in culture for an additional 72 h, followed by extraction of DNA and isolation of the newly synthesized plasmids by *Dpn*I digestion. This *Dpn*I treatment was performed to eliminate unreplicated parental strands that still carried the Dam methylation pattern generated during bacterial amplification of the template (*28*). Finally, transformations of *E. coli* strain DH10B were used to determine the efficiency by which the viral construct was replicated in human fibroblasts. The quantitative loss of plasmids due to replication inhibition by UV damage was calculated from the amounts of *Dpn*I-resistant progeny obtained with irradiated pS189 divided by the corresponding progeny obtained in parallel transfections with unirradiated pS189 controls.

Mean ratios of at least three independent sets of experiments are shown in Figure 2A. In the NER-deficient XP-A cell line, DNA replication was suppressed in a dose-dependent manner when the pS189 template was previously exposed to UV-C radiation. As expected, NER-proficient fibroblasts restored the replication capacity of UV-irradiated vectors because DNA synthesis is facilitated by prior excision of bulky lesions. Interestingly, the extent of reactivation remained unchanged in a direct comparison between methylated and unmethylated substrates, indicating that the human NER system was able to process UV-damaged plasmids even when all cytosines at CpG sites were replaced with 5-methylcytosines. Similar results were obtained with B[*a*]P diol epoxide-damaged shuttle vectors, confirming that reactivation of the viral template is dependent on prior excision of bulky lesions (Figure 2B). In this case, however, the reactivation in NER-proficient fibroblasts was reduced when the vectors were methylated before exposure to the genotoxic agent. For example, we observed that replication efficiency was decreased to 35−40% of the undamaged control when the unmethylated templates were treated with 60 μM B[*a*]P diol epoxide. The same degree of inhibition had previously been detected when the methylated vector was treated with the lower diol epoxide concentration of 40 μM. Nevertheless, replication of the methylated vector was not suppressed to the same extent as in XP-A cells, demonstrating that NER enzymes were still active on B[*a*]P adducts located in methylated substrates. Unmethylated and methylated plasmids were replicated with similar efficiencies in NER-deficient XPA cells (Figure 2B), indicating that the observed difference is due to modulation of NER activity and not to changes in other mechanisms such as replicative bypass.

The experiments performed in intact cells are complicated by the possibility that 5-methylcytosines could be removed from substrate DNA after transfections. Alternatively, unmethylated plasmid DNA may be rapidly methylated following transfection into mammalian cells. In both cases, it would not be possible to compare repair efficiencies because the substrates may become either completely demethylated or, alternatively, completely methylated. We took advantage of the Mcr and Mrr restriction system to rule out these scenarios. It is well-known that mammalian DNA containing 5-methylcytosines at CpG dinucleotides is subject to Mcr and Mrr digestion in *E. coli* (*29*). When the Mcr^- Mrr^- strain DH10B was used to determine replication efficiency, the DNA isolates from each 35 mm well of human fibroblasts (transfected with 0.25 μg of pS189 vector) yielded 10^4-10^5 bacterial colonies, regardless of whether the input DNA was methylated. The same recovery was found when unmethylated pS189 vectors were transfected into human fibroblasts, and replication efficiency was determined by transformation of Mcr^+ Mrr^+ strain DH5α. However, a 50-fold reduction of colony yields was observed when human fibroblasts were transfected with methylated pS189, and replication efficiency was again tested by transformation of Mcr^+ Mrr^+ strain DH5α. Degradation of parental DNA could not account for this reduction in transformation efficiency because, in all

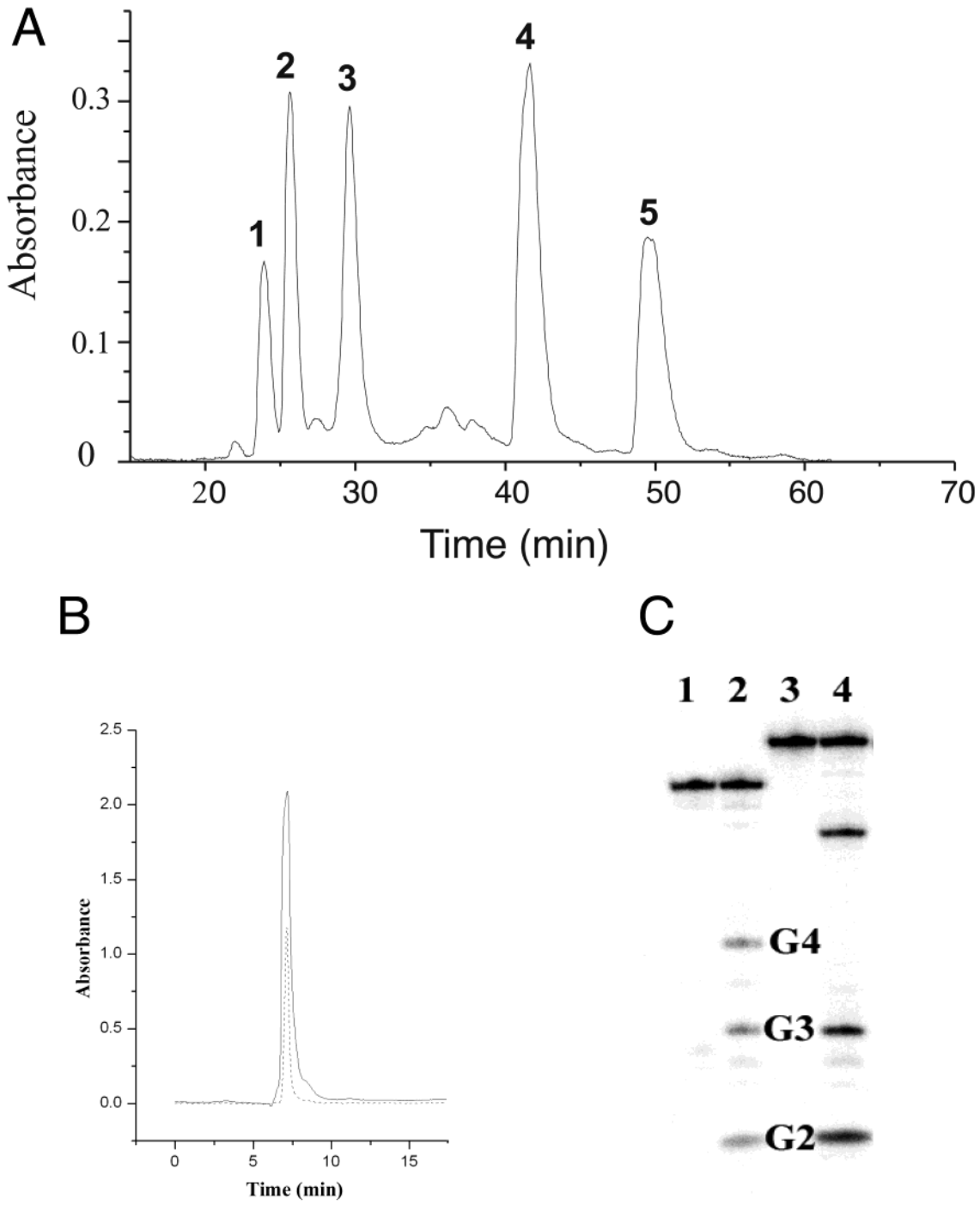

FIGURE 3: Purification and characterization of modified oligonucleotides. (A) Typical reverse-phase elution profile of a reaction mixture containing modified 5′-$G_1TG_2[^mC]G_3TG_4TTTCC$-3′ oligonucleotides resulting from incubation with racemic *anti*-B[*a*]P diol epoxide. Fractions 1−5 were collected and further purified by HPLC [fraction 4 contained the desired (+)-*trans*-*anti*-B[*a*]P−dG adduct at the p53 mutation hot spot G_3]. (B) HPLC elution profile of the purified oligonucleotide 5′-$G_1TG_2CG_3TG_4TTTCC$-3′ with a (+)-*trans*-*anti*-B[*a*]P−dG adduct at position G_3. The solid line is absorbance monitored at 260 nm; the dotted line is fluorescence of the aromatic B[*a*]P residue determined at 400 nm (excitation at 350 nm). (C) Representative Maxam−Gilbert analysis of the same 5′-$G_1TG_2CG_3TG_4TTTCC$-3′ sequence with the (+)-*trans*-*anti*-B[*a*]P-dG adduct at position G_4: lane 1, reaction of unmodified 12-mer oligonucleotide without sequencing; lane 2, Maxam−Gilbert reaction with unmodified 12-mer; lane 3, reaction of (+)-*trans*-*anti*-B[*a*]P−dG adduct without sequencing; and lane 4, Maxam−Gilbert reaction with oligonucleotides containing the (+)-*trans*-*anti*-B[*a*]P−dG adduct.

cases, unreplicated template strands were removed by *Dpn*I digestion before bacterial transformations. Instead, the reduced colony number following Mcr and Mrr restriction in DH5α indicates that SV40 replication products are processed in human cells in a selective manner such that methylated SV40 templates yield methylated daughter strands, whereas in the absence of 5-methylcytosines in parental DNA, the newly synthesized daughter strands remain unmethylated. These results imply that the particular methylation status of transfected plasmids is largely preserved in human fibroblasts.

Excision of a B[a]P Diol Epoxide Adduct in HeLa Cell Extracts. The previous results showed that repair of UV radiation products remains efficient at a global level despite

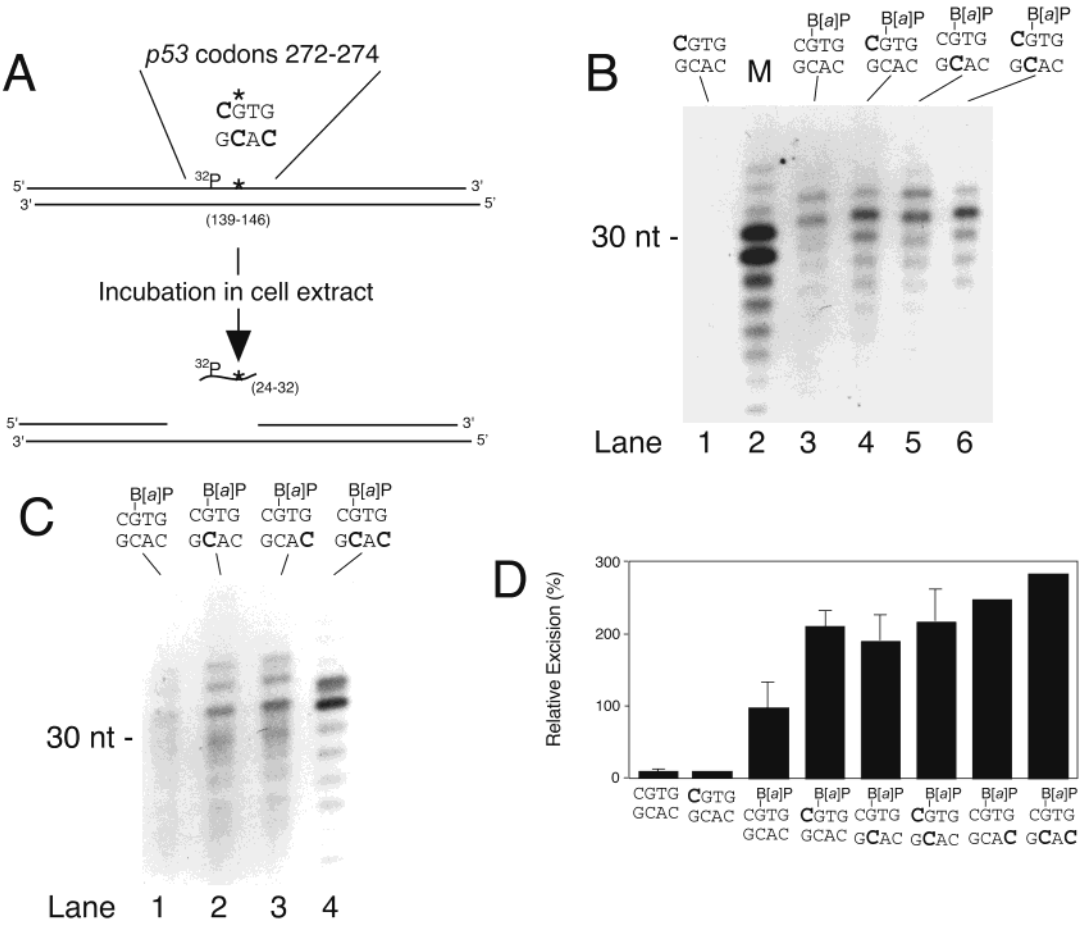

FIGURE 4: Determination of local human NER activity in the *p53* codon 273 sequence (5′-CGT-3′). (A) General scheme illustrating the oligonucleotide excision assay in cell extracts. A single adducted guanine is denoted with the asterisk. The cytosine bases targeted for methylation are shown in bold. (B) Autoradiogram of a representative polyacrylamide gel showing the characteristic oligonucleotide products elicited by excision of a (+)-*trans*-*anti*-B[*a*]P−N^2-dG adduct from the *p53* codon 273 context. A shorter exposure of the upper part of the gel was used to confirm that all reaction mixtures contained the same overall amounts of radioactive substrate (0.2 nM, 75 000 dpm). The methylated cytosine bases are indicated in bold: lane 1, undamaged control substrate; and lane 2, excision of a site-specific (+)-*cis*-*anti*-B[*a*]P−N^2-dG adduct, generating marker oligonucleotides (M) of 29−31 residues. (C) Stimulation of (+)-*trans*-*anti*-B[*a*]P−N^2-dG excision by 5-methylcytosines (lanes 2−4). Lane 1 shows a control reaction with the unmethylated substrate. (D) Quantitative evaluation of two or three independent experiments showing that the presence of 5-methylcytosines resulted in a nearly 3-fold stimulation of excision activity. Standard deviations are indicated for the data calculated from three separate experiments. The remaining results represent mean values of two independent assays.

the presence of methylated CpG dinucleotides. In contrast, the viral reactivation assay suggested that excision of B[*a*]P adducts may be affected to some extent by the presence of 5-methylcytosines. This observation prompted us to examine possible effects of cytosine methylation on B[*a*]P excision in more detail using the human *p53* codon 273 context as a model sequence for *in vitro* NER reactions. A synthetic oligonucleotide (5′-$G_1TG_2CG_3TG_4TTTCC$-3′) with the sequence corresponding to codons 272−274 of the nontranscribed strand in the *p53* gene was exposed to genotoxic B[*a*]P diol epoxide derivatives. This reaction was repeated with the same sequence containing 5-methylcytosine in the CpG site of codon 273 (5′-CG_3T-3′). The resulting products were chromatographically fractionated (Figure 3A) to isolate singly modified oligonucleotides (Figure 3B), in which the quantitatively most abundant (+)-*trans*-*anti*-B[*a*]P−N^2-dG adduct was targeted to the guanine base of codon 273. This method yielded pure preparations of site-specific and stereochemically defined B[*a*]P−dG adducts in the target sequence (*23*). The precise localization of the adduct in each oligonucleotide preparation was established by Maxam−Gilbert analysis (Figure 3C), where cleavage at the modified guanine yields a fragment that has a slower electrophoretic mobility because of the presence of the B[*a*]P residue (lane 4).

The modified oligonucleotides were labeled with [γ-^{32}P]-ATP at the 5′ end and ligated with five other oligomers to produce double-stranded DNA substrates ∼150 base pairs in length that contain an internal radiolabel in the vicinity of the adduct (Figure 4A). These double-stranded fragments were incubated in a standard HeLa cell extract that is proficient in NER activity when supplemented with ATP and deoxyribonucleotide triphosphates (*16*). After incubation for 40 min, radioactive oligonucleotide products generated by the NER enzymes were separated from substrate DNA on denaturing polyacrylamide gels and visualized by autoradiography.

A site-specific (+)-*trans*-*anti*-B[*a*]P−N^2-dG adduct located in the *p53* codon 273 context was excized in human cell extracts, yielding characteristic oligomeric products (Figure 4B, lanes 3−6). A parallel reaction with the (+)-*cis*-*anti*-B[*a*]P−N^2-dG isomer in the sequence 5′-TCGC-3′

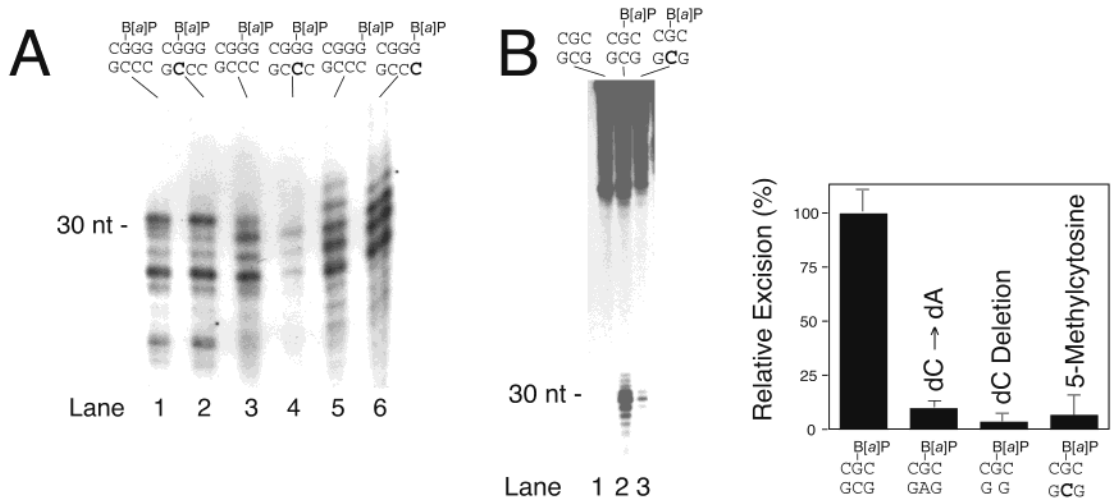

FIGURE 5: Differential effects of 5-methylcytosines on site-specific human NER activity. (A) Excision of a (+)-*trans*-*anti*-B[*a*]P−N^2-dG adduct located at different positions in a run of guanines. In lanes 2, 4, and 6, the cytosine opposite the lesion was replaced with 5-methylcytosine. A shorter exposure of the upper part of the gel was used to confirm that all reaction mixtures contained the same overall amounts of radioactive substrate (0.2 nM, 75 000 dpm). (B) Excision of a (+)-*cis*-*anti*-B[*a*]P−N^2-dG adduct located in the sequence 5′-CGC-3′. In lane 3, the cytosine opposite the adduct was replaced with 5-methylcytosine. The resulting inhibitory effect is comparable to the previously determined suppression of repair activity generated by a base replacement or a nucleotide deletion at the same site (*25*).

(*25*) provided appropriate markers for confirming that the released oligomers displayed the expected size range of 24−32 nucleotides (lane 2). In comparison to this (+)-*cis* marker, the (+)-*trans*-*anti*-B[*a*]P−N^2-dG adduct was excized with low efficiency (lane 3). Unexpectedly, this target adduct was removed from methylated sequences (lanes 4−6) more efficiently than from the corresponding unmethylated substrate (lane 3). Even more surprisingly, approximately the same stimulatory effect was observed regardless of whether a single 5-methylcytosine substitution was introduced into the CpG dinucleotide of the damaged strand (lane 4), or into the opposite CpG of the undamaged strand (lane 5). Stimulation of NER activity was maintained when both strands carried the 5-methylcytosine substitution simultaneously (lane 6). No excision was detected after incubation of cell extracts with methylated but undamaged control substrates (lane 1).

The observation that a 5-methylcytosine residue in the undamaged strand induces an effect similar to that of a single methylation near the adduct in the damaged strand prompted us to further explore the role of cytosine methylation in regulating NER activity. In fact, this finding allows us to perform additional assays without the laborious synthesis and purification of DNA oligonucleotides that contain both an adduct and a methylated residue in the same strand. Thus, excision of the (+)-*trans*-*anti*-B[*a*]P−N^2-dG lesion was reexamined using independent substrate and HeLa cell extract preparations with the following results. First, the local increase in NER activity due to a single 5-methylcytosine substitution across the lesion was confirmed (Figure 4C, lane 2). Second, this stimulation was also observed when another neighboring cytosine in the undamaged strand was methylated (lane 3). Third, excision of the (+)-*trans*-*anti*-B[*a*]P−N^2-dG adduct was further enhanced when both cytosines across the lesion carried a methyl group (lane 4). The quantitative densitometric analysis is plotted in Figure 4D.

DNA excision repair in response to a B[*a*]P−N^2-dG adduct in the *p53* codon 273 sequence context was stimulated by methylation (Figure 4), while the viral reactivation assays suggested a modest decrease in NER efficiency following substrate methylation (Figure 2). These apparently conflicting results prompted us to use a series of (+)-*trans*-*anti*-B[*a*]P−N^2-dG adducts in a different target sequence to further explore the effect of 5-methylcytosines on NER activity. The sequence 5′-CGGG-3′ was chosen because, due to the presence of contiguous guanines, it constitutes a hot spot for B[*a*]P diol epoxide-induced mutagenesis (*30*). Again, we exploited the observation that a single methylated residue near the damage may be sufficient to induce detectable effects.

Three different oligonucleotides were isolated carrying a (+)-*trans*-*anti*-B[*a*]P−N^2-dG adduct in the first, second, or third guanine of the target sequence. In each case, we examined how a single 5-methylcytosine residue in the complementary strand opposite the adduct may regulate human NER activity in cell extracts. In contrast to the results obtained with the *p53* codon 273 sequence, methylation of the CpG site across the bulky adduct on the first guanine failed to stimulate NER activity (Figure 5A, lanes 1 and 2). Also, we reproducibly observed a marked inhibition of NER activity when a 5-methylcytosine was situated opposite the adduct on the second guanine of the target sequence (lanes 3 and 4). A weak stimulation of excision activity was noted when the 5-methylcytosine residue was located across the adduct on the third guanine of the sequence (lanes 5 and 6).

Finally, the (+)-*cis*-*anti*-B[*a*]P−N^2-dG standard in the sequence 5′-TCGC-3′ was subjected to the same analysis. Surprisingly, excision of this bulky adduct was strongly inhibited by the presence of a 5-methylcytosine residue in the DNA substrate (Figure 5B). The quantitative evaluation showed that the addition of a single methyl to the cytosine residue opposite the lesion was able to induce an inhibitory effect similar to that of major structural changes, including, for example, a cytosine to adenine replacement or a deletion of the entire dCMP residue opposite the lesion (Figure 5B). These findings indicate that DNA methylation induces variable effects on human NER activity ranging from stimulation to strong inhibition.

DISCUSSION

Most missense mutations in the human *p53* gene are clustered in highly conserved sequence blocks spanning exon 5 to exon 8 (*31*−*34*). For example, the *p53* mutational spectrum in smoking-associated lung tumors is characterized by G to T transversions at preferential sites of codons 157 (exon 5), 248 (exon 7), and 273 (exon 8). The majority of these transversions are targeted to the guanine residue in the nontranscribed sequence, due to the slower repair of DNA adducts in the nontranscribed strand compared to the more efficient removal of the same lesions from the transcribed strand (*35*). The primary distribution of B[*a*]P diol epoxide-induced DNA damage, mapped at nucleotide resolution, provided a direct link between the genotoxic activity of a major tobacco smoke component and the induction of lung cancer in humans (*36*). In fact, preferential adduct formation has been observed at the same guanine positions in codons 157, 248, and 273 that are also mutational hot spots in lung tumors. This selectivity for binding to specific sites is lost when B[*a*]P diol epoxides are reacted with unmethylated *p53* sequences (*6*, *37*), indicating that constitutive methylation of the *p53* gene in human tissues (*38*−*40*) is an important prerequisite for the striking codon selectivity of B[*a*]P lesions.

The genotoxic (+)-*anti*-B[*a*]P diol epoxide metabolite generates primarily (+)-*trans*-*anti*-B[*a*]P−N^2-dG adducts with a minor proportion of (+)-*cis*-*anti*-B[*a*]P−N^2-dG isomers (*41*). In human cells, Denissenko et al. (*35*) found that these B[*a*]P−N^2-dG adducts are removed from codon 273 of the nontranscribed *p53* strand with a half-life of 10−15 h. Because all mutational hot spots of the human *p53* gene were methylated in the examined cell line, it has not been possible to determine if the excision rate in this critical context may be influenced by the local degree of CpG methylation. However, early stages of tumor progression have been shown to involve widespread DNA hypomethylation (*42*), perhaps affecting the repair susceptibility of particular genes. Therefore, we have targeted the (+)-*trans*-*anti*-B[*a*]P−N^2-dG adduct to a synthetic oligonucleotide that contains the same nontranscribed sequence extending from codon 272 to codon 274 of the *p53* gene. The resulting substrate was subjected to repair in a standard *in vitro* NER assay. Unexpectedly, excision of the B[*a*]P−N^2-dG adduct from *p53* codon 273 was stimulated by 5-methylcytosine substitutions, thereby reducing significantly the half-life of this polycyclic aromatic hydrocarbon lesion in the target sequence.

The addition of a methyl group to pyrimidines is able to change the conformational properties of B[*a*]P adducts, thereby inducing profound effects on the degree of local base displacement (*7*, *43*). Thus, improved repair of the (+)-*trans*-*anti*-B[*a*]P−N^2-dG adduct located in a methylated target sequence is likely to result from alterations in the damage-induced DNA distortion, resulting in the lesion being more susceptible to recognition by the NER complex. The (+)-*cis*-*anti*-B[*a*]P−N^2-dG isomer exemplifies the opposite response involving suppression of excision activity, possibly mediated through the generation of a local DNA distortion that is less amenable to recognition by the NER complex. Several previous reports indicated that the efficiency of bulky lesion removal by nucleotide excision is modulated by the base pairing properties of the damaged site. For example, the local base pair geometry at B[*a*]P adducts can be regulated by changing the predominant *trans* conformation to the rare *cis* isomer (*25*), by replacing the B[*a*]P adduct with benzo[*c*]phenanthrene (*44*), by substituting the base opposite the adduct in the undamged strand (*25*), or by deleting the entire nucleotide opposite the lesion (*45*). All these substrate manipulations alter the degree by which Watson−Crick hydrogen bonding is perturbed and have been shown to induce large changes in NER efficiency (*25*, *44*, *45*). The replacement of cytosine with 5-methylcytosine near an adducted base also alters the local strand pairing capacity and, hence, provides another way to manipulate NER rates. For example, Huang et al. (*43*) revealed a striking conformational change when a *trans* adduct of B[*a*]P diol epoxide is flanked by a methylated cytosine. In the *in vitro* assays of this study, cytosine methylation generated a surprising spectrum of responses, ranging from stimulation to inhibition of NER activity, presumably because each 5-methylcytosine substitution produces unpredictable changes in the local structure, which may depend on the sequence context, the type of adduct, its stereochemical conformation, and the position of the cytosine residue relative to the target adduct.

Our study indicates that CpG methylation not only modulates the pattern of adduct formation but also regulates adduct removal by either stimulating or inhibiting NER activity in a site-specific manner. These variable site-specific effects appear to be mutually compensated in more complex substrates such that reactivation of damaged viral constructs in human cells was either not affected at all (as in the case of UV damage) or only moderately affected (as in the case of B[*a*]P adducts) by substrate methylation. Successful overall repair of methylated SV40-based vectors is not the simple result of intracellular demethylation reactions. In fact, Graessmann et al. (*46*) have previously shown that SV40 genomes extracted from human cells retain the methylation pattern of input DNA. Also, we observed in our study that methylation of parental DNA in the viral vector is at least partially maintained in the newly synthesized daughter strands, consistent with the assumption that the viral construct is not demethylated after transfection in human cells.

ACKNOWLEDGMENT

We thank Dr. M. Seidman for plasmid pS189 and Dr. A. Seidel for a gift of B[*a*]P diol epoxide.

REFERENCES

1. Razin, A. (1998) *EMBO J. 17*, 4905−4908.
2. Turker, M. S. (1999) *Semin. Cancer Biol. 9*, 329−337.
3. Bestor, T. H. (2000) *Hum. Mol. Genet. 9*, 2395−2402.
4. Harvey, R. G. (1991) *Polycyclic Aromatic Hydrocarbons: Chemistry and Carcinogenesis*, Cambridge University Press, Cambridge, United Kingdom.
5. Szeliga, J., and Dipple, A. (1998) *Chem. Res. Toxicol. 11*, 1−11.
6. Denissenko, M. F., Chen, J. X., Tang, M. S., and Pfeifer, G. P. (1997) *Proc. Natl. Acad. Sci. U.S.A. 94*, 3893−3898.
7. Weisenberger, D. J., and Romano, L. J. (1999) *J. Biol. Chem. 274*, 23948−23955.
8. Miller, E. C. (1978) *Cancer Res. 38*, 1479−1496.
9. Kriek, E., and Westra, J. G. (1979) in *Chemical Carcinogens and DNA* (Grover, P. L., Ed.) Vol. 2, pp 1−28, CRC Press, Boca Raton, FL.
10. Chen, J. X., Zheng, Y., West, M., and Tang, M. S. (1998) *Cancer Res. 58*, 2070−2075.

11. Tommasi, S., Denissenko, M. F., and Pfeifer, G. P. (1997) *Cancer Res. 57*, 4727−4730.
12. Friedberg, E. C., Walker, G. C., and Wolfram, S. (1995) *DNA Repair and Mutagenesis*, ASM Press, Washington, DC.
13. Sancar, A. (1996) *Annu. Rev. Biochem. 65*, 43−81.
14. Lindahl, T., and Wood, R. D. (1999) *Science 286*, 1897−1905.
15. de Boer, J., and Hoeijmakers, J. H. (2000) *Carcinogenesis 21*, 453−460.
16. Huang, J. C., Svoboda, D. L., Reardon, J. T., and Sancar, A. (1992) *Proc. Natl. Acad. Sci. U.S.A. 89*, 3664−3668.
17. Mu, D., Hsu, D. S., and Sancar, A. (1996) *J. Biol. Chem. 271*, 8285−8294.
18. Wood, R. D. (1997) *J. Biol. Chem. 272*, 23465−23468.
19. Shivji, M. K., Podust, V. N., Hubscher, U., and Wood, R. D. (1995) *Biochemistry 34*, 5011−5017.
20. Reardon, J. T., Thompson, L. H., and Sancar, A. (1997) *Nucleic Acids Res. 25*, 1015−1021.
21. Seidman, M. (1989) *Mutat. Res. 220*, 55−60.
22. Geacintov, N. E., Cosman, M., Mao, B., Alfano, A., Ibanez, V., and Harvey, R. G. (1991) *Carcinogenesis 12*, 2099−2108.
23. Mao, B., Xu, J., Li, B., Margulis, L. A., Smirnov, S., Ya, N. Q., Courtney, S. H., and Geacintov, N. E. (1995) *Carcinogenesis 16*, 357−365.
24. Maxam, A., and Gilbert, W. (1997) *Methods Enzymol. 65*, 499−504.
25. Hess, M. T., Gunz, D., Luneva, N., Geacintov, N. E., and Naegeli, H. (1997) *Mol. Cell. Biol. 17*, 7069−7076.
26. Matsunaga, T., Mu, D., Park, C. H., Reardon, J. T., and Sancar, A. (1995) *J. Biol. Chem. 270*, 20862−20869.
27. Manley, J. L., Fire, A., Cano, A., Sharp, P. A., and Gefter, M. L. (1980) *Proc. Natl. Acad. Sci. U.S.A. 77*, 3855−3859.
28. Wang, Y. C., Maher, V. M., and McCormick, J. J. (1991) *Proc. Natl. Acad. Sci. U.S.A. 88*, 7810−7814.
29. Raleigh, E. A. (1992) *Mol. Microbiol. 6*, 1079−1086.
30. Rodriguez, H., and Loechler, E. L. (1993) *Carcinogenesis 14*, 373−383.
31. Hsu, I. C., Metcalf, R. A., Sun, T., Welsh, J. A., Wang, N. J., and Harris, C. C. (1991) *Nature 350*, 427−428.
32. Bressac, B., Kew, M., Wands, J., and Ozturk, M. (1991) *Nature 350*, 429−431.
33. Pfeifer, G. P., and Holmquist, G. P. (1997) *Biochim. Biophys. Acta 1333*, M1−M8.
34. Hainaut, P., and Pfeifer, G. P. (2001) *Carcinogenesis 22*, 367−374.
35. Denissenko, M. F., Pao, A., Pfeifer, G. P., and Tang, M. (1998) *Oncogene 16*, 1241−1247.
36. Denissenko, M. F., Pao, A., Tang, M., and Pfeifer, G. P. (1996) *Science 274*, 430−432.
37. Tang, M. S., Zheng, J. B., Denissenko, M. F., Pfeifer, G. P., and Zheng, Y. (1999) *Carcinogenesis 20*, 1085−1089.
38. Tornaletti, S., and Pfeifer, G. P. (1995) *Oncogene 10*, 1493−1499.
39. Rideout, W. M., Coetzee, G. A., Olumi, A. F., and Jones, P. A. (1990) *Science 249*, 1288−1290.
40. Magewu, A. N., and Jones, P. A. (1994) *Mol. Cell. Biol. 14*, 4225−4232.
41. Geacintov, N. E., Cosman, M., Hingerty, B. E., Amin, S., Broyde, S., and Patel, D. J. (1997) *Chem. Res. Toxicol. 10*, 111−146.
42. Goelz, S. E., Vogelstein, B., Hamilton, S. R., and Feinberg, A. P. (1985) *Science 228*, 187−190.
43. Huang, X., Colgate, K. C., Kolbanovskiy, A., Amin, S., and Geacintov, N. E. (2002) *Chem. Res. Toxicol. 15*, 438−444.
44. Buterin, T., Hess, M. T., Luneva, N., Geacintov, N. E., Amin, S., Kroth, H., Seidel, A., and Naegeli, H. (2000) *Cancer Res. 60*, 1849−1856.
45. Buterin, T., Hess, M. T., Gunz, D., Geacintov, N. E., Mullenders, L. H., and Naegeli, H. (2002) *Cancer Res. 62*, 4229−4235.
46. Graessmann, M., Graessmann, A., Wagner, H., Werner, E., and Simon, D. (1983) *Proc. Natl. Acad. Sci. U.S.A. 80*, 6470−6474.

BI0268504